

# Time-Resolved IR Spectroscopy of *N*-Methylthioacetamide: *Trans* → *Cis* Isomerization upon $n-\pi^*$ and $\pi-\pi^*$ Excitation and *Cis* → *Trans* Photoreaction

Valentina Cervetto, Harald Bregy, Peter Hamm, and Jan Helbing\*

Physikalisch-Chemisches Institut, Winterthurerstrasse 190, CH-8057 Zürich, Switzerland

Received: May 10, 2006; In Final Form: August 21, 2006

Time-resolved infrared spectroscopy was used to study the photoisomerization of *N*-Methylthioacetamide (NMTAA) in D<sub>2</sub>O in both the *cis* → *trans* and the *trans* → *cis* direction upon selective excitation of the  $n-\pi^*$  (S<sub>1</sub>) and  $\pi-\pi^*$  (S<sub>2</sub>) electronic transitions. While isomerization and the return to the ground state takes place on two distinct time scales ( $\leq 8$  ps,  $\sim 250$  ps) upon  $\pi-\pi^*$  excitation of both *cis*- and *trans*-NMTAA in D<sub>2</sub>O, ground state recovery is only observed on the slower time scale upon  $n-\pi^*$  excitation. The quantum efficiency for *trans* → *cis* isomerization is 30–40%, independent of the electronic state excited, while the *cis* → *trans* isomerization proceeds with a 60–70% quantum efficiency. These results support a mechanism by which isomerization takes place via one common intermediate state independent of electronic excitation energy and initial conformation.

## I. Introduction

Thiopeptides are peptides where sulfur replaces oxygen in one or more of the backbone carbonyl groups. This one atom substitution significantly lowers the electronic transition frequency of the  $\pi-\pi^*$  and  $n-\pi^*$  transitions, making it possible to selectively excite and isomerize one peptide unit from the *trans* to the metastable *cis* conformation. Growing interest in the photoisomerization of thiopeptides in recent years is linked to the hope to control enzymatic activity<sup>1–3</sup> and to use isomerization of the thiopeptide bond to induce and time-resolve conformational dynamics in essentially native peptides.<sup>4,5</sup> *N*-Methylthioacetamide (NMTAA), the thio-substituted analogue of *N*-methylacetamide (NMA), is the simplest photoswitchable molecule with a thioamide bond. It can be regarded as the molecular switch in larger thiopeptides and its photoisomerization has first been studied by Tasumi and co-workers.<sup>6–8</sup> In an earlier publication, we have reported time-resolved visible and infrared absorption measurements following excitation of *trans*-NMTAA to the S<sub>2</sub> ( $\pi-\pi^*$ ) state, and proposed an isomerization mechanism with the help of ab initio minimum energy path calculations by De Vico and Olivucci.<sup>4</sup> In that work, we observed two distinct time scales, of approximately 8 and 250 ps, for both the formation of *cis*-NMTAA and the recovery of *trans*-NMTAA in the electronic ground state with a total quantum efficiency for *trans* → *cis* isomerization of 30–40%.

Pump–probe experiments in the visible clearly showed that the long time constant corresponds to the decay of an electronically excited state, which can be identified with either the lowest-lying singlet (S<sub>1</sub>) or triplet state (T<sub>1</sub> or T<sub>2</sub>).<sup>4,5</sup> According to the ab initio calculations the potential energy surface of all three states can be reached by ultrafast S<sub>2</sub>–S<sub>1</sub> decay or intersystem crossing, and they are essentially flat along the torsional coordinate along which isomerization takes place. S<sub>1</sub> or T<sub>1</sub> surfaces are connected to the electronic ground state via four conical intersections (CI) S<sub>1</sub>/S<sub>0</sub> or intersystem crossing points (ICS), located at a few kJ/mol above the respective potential minima. Relaxation via three of these CIs (or ICSs)

was found to lead back to the *trans* ground state and one to the *cis* ground state, suggesting that the outcome of the photoreaction is determined on the excited-state surface. Because isomerization occurs with similar quantum efficiency on the slow and the fast time scale, we proposed that there is a competition between immediate S<sub>1</sub>–S<sub>0</sub> relaxation of the initially hot excited state population and cooling in the electronically excited states. However we could not exclude that the two time scales are due to competition between different pathways involving the triplet and singlet states. Indeed, an alternative interpretation of the observed branching has recently been proposed by Satzger et al.<sup>5</sup> These authors postulate an inversion of the triplet state ordering and suggest competition between fast intersystem crossing from the <sup>3</sup>n- $\pi$  triplet state to the electronic ground state and triplet–triplet (<sup>3</sup>n $\pi$  → <sup>3</sup> $\pi\pi$ ) relaxation.

Here, to better explore the electronic relaxation mechanism leading to isomerization, we compare the dynamics of *trans* → *cis* photoisomerization after excitation to the S<sub>2</sub> and S<sub>1</sub> states in deuterated water. In addition, we present a method to accumulate and selectively excite *cis*-NMTAA and follow the *cis* → *trans* reaction in real time. The solvent dependence of the reaction was tested by carrying out complementary measurements in deuterated acetonitrile (CD<sub>3</sub>CN).

## II. Experimental Setup

The measurements were carried out on 200–300 mM solutions of NMTAA in D<sub>2</sub>O or CD<sub>3</sub>CN, which were circulated in a flow cell (2 mm CaF<sub>2</sub> windows, spaced 50  $\mu$ m apart) at a rate sufficient to ensure the complete exchange of sample volume between excitation pulses.<sup>9</sup> Femtosecond pulses for IR measurements (1 kHz, 700  $\mu$ J/pulse, 80 fs) were obtained from an amplified titanium-sapphire laser system (Spectra Physics), operating either near 800 or 840 nm. The mid-infrared pulses in the 1200–1600 cm<sup>-1</sup> range (100 fs, 250 cm<sup>-1</sup> bandwidth) were produced in a home-built double-stage optical parametric amplifier (OPA) followed by frequency mixing in a AgGaS<sub>2</sub> crystal.<sup>10</sup> The IR pulses were split into two parts (of 50 nJ each). One part (the probe pulse) was

\* Corresponding author. E-mail: email: j.helbing@pci.unizh.ch.

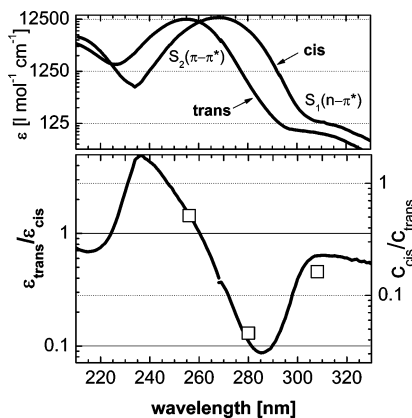


**Figure 1.** a) Logarithmic plot of the UV-absorption of *trans* – and *cis*-NMTAA in water. b) Logarithmic plot of the absorption ratio  $\epsilon_{\text{trans}}/\epsilon_{\text{cis}}$  (left scale). The squares (right scale) represent the concentration ratio  $C_{\text{cis}}/C_{\text{trans}}$  in photo equilibrium, measured by  $^1\text{H}$  NMR (see Table 1 in ref. [4]).

overlapped with the UV pump pulse in the sample cell. The second part was used as a reference beam to correct for intensity fluctuations and crossed the flow cell approximately  $500\ \mu\text{m}$  further upstream. Both IR beams were dispersed in a spectrometer and detected with a double MCT array ( $2 \times 32$  pixels) on a single shot basis with  $3\ \text{cm}^{-1}$  resolution. The UV pump light at  $280\ \text{nm}$  was generated by frequency tripling of the  $840\ \text{nm}$  IR light in two BBO crystals, the third harmonic beam was then isolated by dielectric mirrors, and the UV pulses were stretched to  $1.4\ \text{ps}$  duration by guiding them through  $15\ \text{cm}$  of fused silica. Pulses at  $308\ \text{nm}$  ( $1.5\ \mu\text{J}/\text{pulse}$ ) were obtained by sum frequency mixing the  $500\ \text{nm}$  output ( $7\ \mu\text{J}/\text{pulse}$ ) of a home-built noncollinear optical parametric amplifier (NOPA) with the  $800\ \text{nm}$  fundamental in a BBO crystal. The pump pulse polarization was rotated by  $90^\circ$  every  $300$  laser shots and data was collected quasi simultaneously for parallel and perpendicular polarization of pump and probe beams. For the investigation of the *cis*  $\rightarrow$  *trans* process a photo equilibrium with a strongly enhanced *cis* concentration was maintained by continuously irradiating the sample with  $20\ \text{mW}$  UV light at  $248\ \text{nm}$  from a KrF Excimer laser (Lambda Physik,  $10\ \text{Hz}$ ) before and during the measurements (see below).

### III. Results

**A. Outline of the Experiment.** In water at room temperature, the *cis*-NMTAA concentration in thermal equilibrium is only  $1.5\%$ , and *trans*-NMTAA can be selectively excited both to the  $S_2$  ( $260\ \text{nm}$ ), which corresponds to a  $\pi\text{-}\pi^*$  excitation, and the  $S_1$  state (shoulder at  $308\ \text{nm}$ ), which corresponds to a  $n\text{-}\pi^*$  excitation.<sup>4</sup> Because the absorption spectra of the two isomers strongly overlap (see Figure 1a), and photoisomerization takes place in both directions, UV-irradiation can only transfer a fraction of the molecules into the *cis* state before photoequilibrium is established. As shown in Figure 1b) the concentration ratio  $C_{\text{cis}}/C_{\text{trans}}$  (solid squares) in photoequilibrium at different wavelengths is proportional to the ratio of extinction coefficients  $\epsilon_{\text{trans}}/\epsilon_{\text{cis}}$  (solid line). Under continuous irradiation at  $248\ \text{nm}$  we can thus prepare a sample with a *cis* concentration of  $\approx 45\%$ . When this sample is then excited by a short laser pulse at  $282\ \text{nm}$ , where *cis*-NMTAA absorbs 10 times more than *trans*-NMTAA, more than  $90\%$  of the excited molecules are initially in the *cis* configuration. Because this selectivity as a function of pump laser wavelength is not possible for  $S_1$  ( $n\text{-}\pi^*$ ) excitation, *cis*-NMTAA could be selectively excited only to the

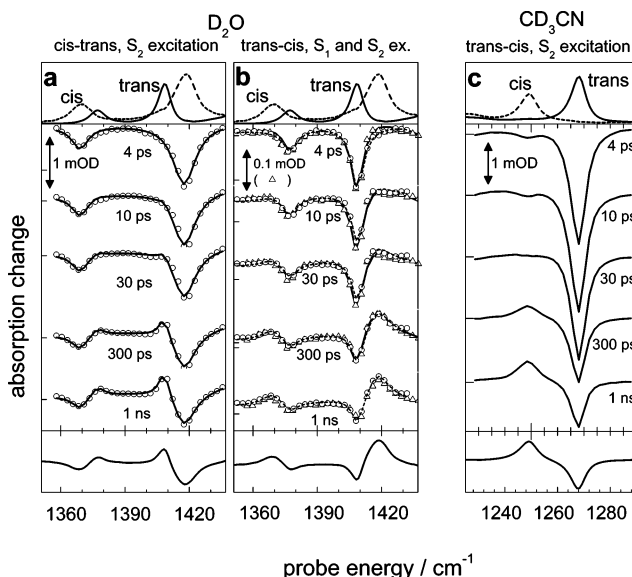


**Figure 2.** Magic angle transient infrared absorption spectra at different time delays: (a)  $282\ \text{nm}$  ( $S_2$ ) excitation of a sample in photoequilibrium, containing  $45\%$  *cis*-NMTAA and  $55\%$  *trans*-NMTAA. Because of the smaller *trans*-absorption at  $280\ \text{nm}$   $> 90\%$  of the excited molecules were originally in the *cis* state; (b)  $258\ \text{nm}$  excitation of the  $S_2$  state of *trans*-NMTAA (open circles, scaled by a factor of  $1/12$ ) and  $308\ \text{nm}$  excitation of the  $S_1$  state of *trans*-NMTAA (open triangles), where dashed ( $S_2$  excitation) and thick black lines ( $S_1$  excitation) show least-squares fits using a linear combination of the *cis* and the *trans* FTIR absorption spectra (shown at the top); (c)  $266\ \text{nm}$  ( $S_2$ ) excitation of *trans*-NMTAA in  $\text{CD}_3\text{CN}$ , with FTIR absorption spectra (top) and the FTIR difference absorption spectrum (bottom).

$S_2$  state. Also note that the  $n\text{-}\pi^*$  absorption band is shifted to  $345\ \text{nm}$  in  $\text{CD}_3\text{CN}$  and could not be excited with our present setup.

As in our previous study, we chose the spectral range  $1300\text{--}1450\ \text{cm}^{-1}$  to monitor the infrared absorption changes during the isomerization process in  $\text{D}_2\text{O}$ . Two bands, best described as symmetric and antisymmetric stretch motion of the C–C–N–C backbone can be nicely separated for the two isomers. The *trans* band at  $1409\ \text{cm}^{-1}$  is blue-shifted to  $1420\ \text{cm}^{-1}$  in *cis*, while a red-shifted band at  $1365\ \text{cm}^{-1}$  is the counterpart of the *trans* band at  $1377\ \text{cm}^{-1}$  (Figure 2, top). An even better separation of the two isomers is observed in acetonitrile for the C–C–N bending transition, which shifts from  $1268\ \text{cm}^{-1}$  for *trans*-NMTAA to  $1249\ \text{cm}^{-1}$  in the *cis* isomer (Figure 2, top right). This mode cannot be used for time-resolved measurements in  $\text{D}_2\text{O}$  because of solvent absorption.

**B. Time-Resolved Measurements.** Figure 2a shows the transient IR absorption changes at different pump–probe delays for selective excitation of *cis*-NMTAA in  $\text{D}_2\text{O}$  to the  $S_2$  state. Spectra recorded for excitation of *trans*-NMTAA to the  $S_2$  state (open circles) and the  $S_1$  state (open triangles) are compared in Figure 2b. For  $S_2$ -excitation of *trans*-NMTAA in acetonitrile we observe the transients shown in Figure 2c. All data are magic angle signals  $S_{\text{magic}} = (S_{\parallel} + 2S_{\perp})/3$  and are unaffected by rotational diffusion, which takes place with a  $3.7 \pm 0.5\ \text{ps}$  time constant in acetonitrile, compared to  $10.5 \pm 1\ \text{ps}$  in  $\text{D}_2\text{O}$ . The ratio of these values is equal to the ratio of the different solvent viscosities of  $0.357\ \text{cP}$  and  $1.096\ \text{cP}$ ,<sup>11</sup> a result well-known from the diffusion of dye molecules.<sup>12</sup>

*Cis* excitation leads to an instantaneous bleach of the *cis* absorption bands. This bleach subsequently decreases and in parallel new absorption bands grow near the spectral positions of ground state *trans*-NMTAA absorption. The opposite (*trans*-

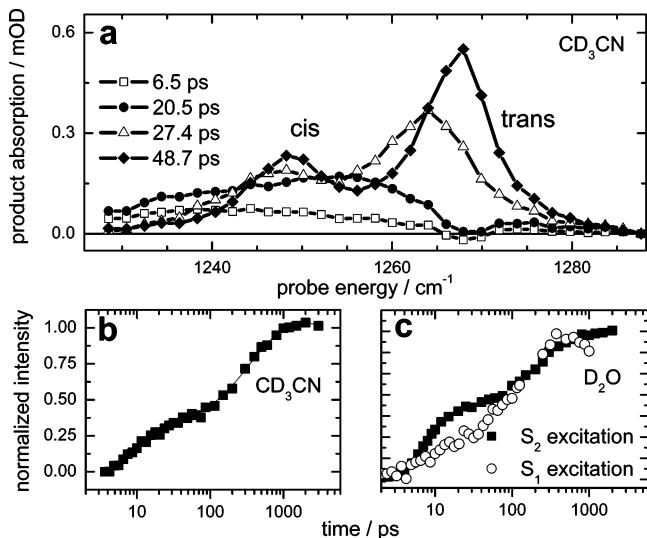


**Figure 3.** (a) Photoinduced vibrational bands of NMTAA in  $\text{CD}_3\text{CN}$  at various delays after excitation of the *trans* form to the  $S_2$  state. The spectra were obtained by subtracting the pure bleaching signal at a pump–probe delay of 2 ps from the pump–probe data of Figure 2c. (b) Integrated area under the peaks in part a. (c) Same as part b but for the stretch bands of NMTAA in  $\text{D}_2\text{O}$ , for  $S_2$  (squares) and for  $S_1$  excitation (open circles), corresponding to the transient of Figure 2b.

bleach followed by the growth of the *cis*-NMTAA bands) is observed for excitation of *trans*-NMTAA, both in  $\text{D}_2\text{O}$  and in  $\text{CD}_3\text{CN}$  (Figure 2, parts b and c). The superposition of the data for  $S_1$  and  $S_2$  excitation of *trans* NMTAA in  $\text{D}_2\text{O}$  in Figure 2b reveals very similar signals. The two sets of data have been scaled to the 4 ps transient and match again perfectly after 300 ps. However, at intermediate delays (10 ps, 30 ps) the bleach of the *trans*-bands appears to be smaller for  $S_2$ -excitation (open circles, dashed line) than for  $S_1$ -excitation (up-triangles, solid line). We show below (Figure 3c), that this small difference is indeed significant and is due to more efficient fast relaxation to the electronic ground state, when the  $S_2$  state is excited. As already discussed in ref.<sup>4</sup> for excitation of *trans*-NMTAA to the  $S_2$ -state, no signals from excited electronic states can be seen. The most probable reason is that the C–N–C stretch- and bending transitions of molecules in the electronically excited state(s) are shifted out of our detection window as the bond order of the thioamide N–C bond is reduced, the nitrogen and carbon centers pyramidalize and the force constants are strongly changed.<sup>4</sup>

The transient spectra in Figure 2 show the difference in absorption between NMTAA molecules after photoexcitation and before they have absorbed a UV photon. However, in the present case we can recover the pure absorption bands of the molecules after photoexcitation by subtracting the transient signals at the earliest time delays. This is possible because in the absence of excited-state absorption bands the pump–probe spectra at delays shorter than 2 ps are exact replica of the ground-state absorption spectra. The resulting signals in the bending region of NMTAA dissolved in acetonitrile are shown in Figure 3a ( $\pi$ – $\pi^*$  excitation of *trans*-NMTAA). Note that these spectra would be observed directly if the photoproduct transitions appeared at a different energy than those of the educt.

A few picoseconds after photoexcitation to the  $S_2$  state a broad absorption band becomes visible to the red of the IR transitions in the electronic ground state. It only gradually narrows as the red shift decreases and eventually develops into well-separated peaks that correspond to absorption bands of completely relaxed ground state *trans*- and *cis*-NMTAA. The time delay after which

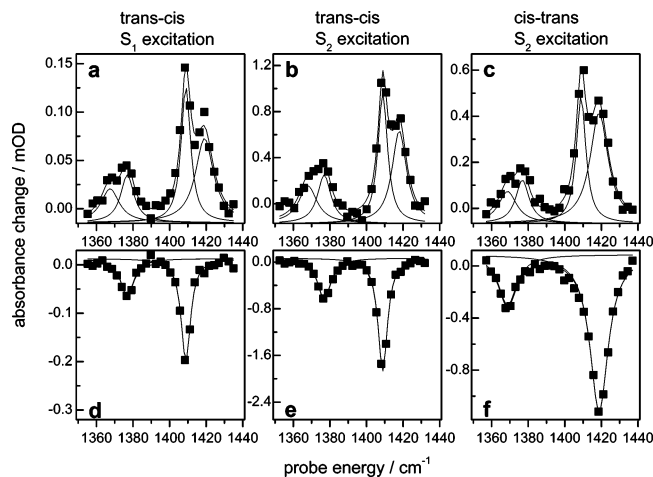
*cis* and *trans* bands can be distinguished depends on the transition. In  $\text{CD}_3\text{CN}$  the bending transitions of the two isomers near  $1260\text{ cm}^{-1}$  are clearly resolved after 30 ps while at the same delay there is still a single band in the stretch region (data not shown). In  $\text{D}_2\text{O}$  a broad band with its center between the *cis* and *trans* ground state symmetric and antisymmetric stretch bands and the two species can be distinguished only after delays longer than 80 ps. Both *cis* and *trans* bands continue to grow between 80 ps and 1 ns, but no further frequency shifts or changes in the *cis*/*trans* intensity ratio are observed.

Figure 3b shows the integrated area (*cis* and *trans*) under the photoinduced absorption peaks of Figure 3a as a function of pump–probe delay. A biphasic growth on a 10 ps and a 350 ps time scale is clearly observed, which reflects the return of excited-state population to the ground-state surface on two time scales. Integrating the corresponding bands in the stretch region near  $1400\text{ cm}^{-1}$  yields very similar results for  $S_2$ -excitation of NMTAA in water (squares in Figure 3c).  $S_2$  excitation of both *cis*- and *trans*-NMTAA leads to a biphasic growth of the integrated signals with time constants of 8–10 and 250 ps. However, a very different situation is encountered upon excitation of the *trans* sample to the  $S_1$  state at 308 nm, where the new absorption features appear to form later (open circles in Figure 3c). In contrast to the two distinct time scales for the ground-state recovery after  $S_2$  excitation, we observe a continuous, slow growth of the photoproduct bands. In the transient spectra of Figure 2b this difference, which is also confirmed by a singular value decomposition analysis, is reflected by the slightly larger bleaching signal at intermediate delays for  $S_1$  excitation.

The initial red-shift and broadening of the vibrational bands of the molecules that reach the electronic ground state on the fast time scale after  $S_2$  excitation is due to anharmonic coupling of these high frequency transitions to a bath of thermally excited low-frequency modes,<sup>13</sup> which take up the excess energy in the molecule during and after electronic relaxation. The subsequent narrowing of the high-frequency bands reflects vibrational cooling in the electronic ground state as the molecule dissipates energy to the solvent on a typical time scale of 10–20 ps. Because the coupling to the low frequency vibrations is mode-specific, spectral changes in the bending mode do not necessarily occur exactly with the cooling time constant.<sup>13</sup> In addition, the diminishing overlap between the *cis* and the *trans* bands in Figure 3a leads to pronounced spectral changes at relatively late delays (20–50 ps). Nevertheless, the observed transients are compatible with exponential cooling dynamics with time constants close to the values extracted from exponential fits to Figure 3, parts b and c (8 ps in  $\text{D}_2\text{O}$ , 13 ps in  $\text{CD}_3\text{CN}$ ). These values only put an upper limit to the time constant of fast electronic decay. For those molecules which reach the electronic ground state on a slower time scale than vibrational cooling, (those excited to the  $S_1$  state and approximately 50% of the molecules excited to  $S_2$ ), on the other hand, the vibrational transitions in the electronic ground state immediately appear as separate *cis* and *trans* bands, and the slow time constant in the IR-signal matches that of the decay of the electronically excited state determined by UV–visible spectroscopy.<sup>4,5</sup>

In the top row of Figure 4, we show the photoproduct spectra in deuterated water for a delay of 2 ns (again obtained by subtracting from the pump–probe data the negative contribution, i.e., the pump–probe spectrum at early delays, which is shown in the bottom row). At the end of the photoreaction the well separated peaks of ground state *trans*- and *cis*-NMTAA directly report on the quantum yields for isomerization. Without





**Figure 4.** (a–c) Photoinduced vibrational bands of NMTAA in  $D_2O$  at long time delays for different excitation conditions and initial conformations. The spectra were obtained by subtracting the pure bleaching signal at a pump–probe delay of 2 ps from the original pump–probe data. Vertical scales are chosen to yield the same height of the trans-peak in all spectra. (d–f) Short time pump–probe spectra (2 ps) that were subtracted from the 2 ns data to produce the top graphs. The relative scales are the same as in the top graphs. Key: (a, d)  $n-\pi^*$  ( $S_1$ ) excitation of *trans*-NMTAA; (b, e)  $\pi-\pi^*$  ( $S_2$ ) excitation of *trans*-NMTAA; (c, f)  $\pi-\pi^*$  ( $S_2$ ) excitation of *cis*-NMTAA.

isomerization, the spectra in the top row would have exactly the same amplitude and shape as the initial bleach signal at early times. However, the amplitude of the trans bands in Figure 4, parts a and b, only amounts to  $\approx 60\%$  of the corresponding bleach signals in Figure 4, parts d and e, indicating a quantum efficiency of isomerization  $\eta \approx 40\%$ . Likewise, the cis bands in Figure 4c contain only  $\approx 40\%$  of the initial cis bleach intensity (Figure 4f) as a result of a  $\approx 60\%$  quantum efficiency for *cis*  $\rightarrow$  *trans* isomerization. This simple argument can be used as long as only one species (*cis* or *trans*) is excited by the pump beam. The bleach signal in the second column of Figure 4 contains contributions from  $\approx 5\%$  of *trans*-NMTAA, which must be taken into account when calculating  $\eta$ . We determine the isomerization quantum yield to be 30–40% in the *trans*–*cis* direction and 60–70% in the *cis*–*trans* direction. The error in the quantum efficiency determination is mainly due to uncertainties in the fits with overlapping (Lorentzian) line shapes. The ratio of quantum efficiencies  $\eta_{\text{cis} \rightarrow \text{trans}} / \eta_{\text{trans} \rightarrow \text{cis}} = 1.5\text{--}2.3$  can be compared to the corresponding ratio of 2.1–3.5 extracted from combined steady-state UV and NMR measurements reported in ref.<sup>4</sup> Thermal *cis*  $\rightarrow$  *trans* relaxation on the ground state surface is too slow to influence either of the measurements significantly. Independent of the comparison with the initial bleach signals, the similarity of the photoproduct signals for  $S_2$  and  $S_1$  excitation of *trans*-NMTAA and  $S_2$ - excitation of *cis*-NMTAA clearly show, that similar ratios of both isomers are formed independently of the initial configuration and excitation wavelength.

## Discussion

Although the transient IR spectra of NMTAA are not sensitive directly to the electronically excited states, our observation of different ground-state recovery following  $n-\pi^*$  ( $S_1$ ) and  $\pi-\pi^*$  ( $S_2$ ) excitation, and comparison of the two different solvents can nevertheless be critically related to the excited-state relaxation mechanism and thiopeptide isomerization.

In a recent publication, Satzger et al. report on a detailed investigation of the excited-state absorption of NMTAA and short secondary thiopeptides by transient UV–visible spectroscopy

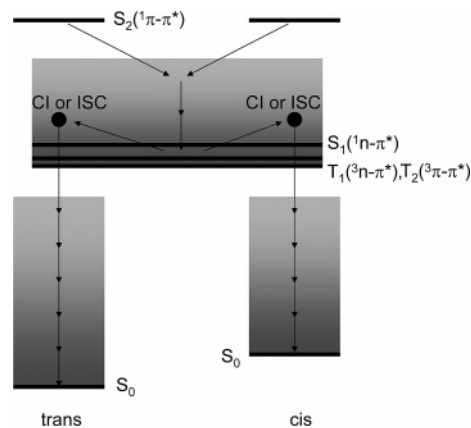


**Figure 5.** Schematic representation of the photoisomerization mechanism of NMTAA, based on the ab initio calculations of ref 4 and the transient IR data presented in this paper. The conical intersections and intersystem crossing points that link the  $S_1$  and the triplet states to the electronic ground state are located *above* the potential energy minima of these excited-state surfaces and are accessed by a diffusive search once the initial excess energy is dissipated.

copy after  $S_2$  excitation.<sup>5</sup> For comparison these authors also report on measurements on thioacetamide (TAA), which does not possess isomers, and a small cyclic thioxoamide ((*S*)-5-thioxopyrrolidine-2-carboxylic acid ethyl ester, CTA), chosen because *trans*–*cis* isomerization is blocked.<sup>5</sup> In all thioxo compounds they observed the long-lived excited-state absorption signal centered near 540 nm (470 nm for CTA and TAA) that had been identified with either the lowest lying singlet or triplet excitation of the thioamide bond in ref 4. It was found to grow on a subpicosecond time scale, with a second  $\approx 4$  ps growth component in NMTAA, CTA, and TAA only. The decay of the excited-state absorption band takes place on a similar time scale as in NMTAA in all isomerizing compounds (from 120 ps in Phe- $\Psi$ [CS–NH]–Ala to 350 ps in the much longer thioxoHis<sup>12</sup>-*S*-peptide (20 amino acids), and 670 ps for CTA). To explain the observed time scales, Satzger et al. proposed a relaxation mechanism governed by ultrafast intersystem crossing from the initially excited  $S_2$ -state ( $^1\pi-\pi^*$ ) to the  $^3n-\pi^*$  triplet state. This spin–flip transition could be strongly enhanced by the simultaneous change of the orbital character (ElSayed’s rule<sup>14</sup>). For the same reason Satzger et al. argued that the  $^3n-\pi^*$  triplet state should quickly relax back to the singlet ground state, giving rise to the fast relaxation channel observed in the transient IR-measurements on NMTAA (Figure 3 and ref 4). In this scheme the long-lived excited state is the  $^3\pi-\pi^*$  triplet state that must have shifted below the  $^3n-\pi^*$  triplet state by polar solvation of the thioamides (see Fig. 4 in reference<sup>5</sup> and Figure 5).

Figure 3c clearly shows that compared to  $S_2$  excitation fewer molecules follow the fast relaxation channel when *trans*-NMTAA is excited to the  $S_1$  state. Indeed, by the ElSayed rule, relaxation via intersystem crossing of  $S_1$  ( $^1n-\pi^*$ ) would preferentially populate  $^3\pi-\pi^*$ , which is the lowest, long-lived state in the scheme proposed by Satzger et al., whereas the fast-decaying  $^3n-\pi^*$  state would be bypassed. Thus, it may be argued that an inversion of the triplet state ordering is sufficient to explain all experimental observations on the photoisomerization dynamics of NMTAA (refs 4 and 5 and this work). For this explanation to be fully consistent with our data, however, polar solvation needs to shift the  $^3n-\pi^*$  state above the  $^3\pi-\pi^*$  state of NMTAA in both water and acetonitrile, where the corresponding singlet states are energetically much further apart. (The  $^1n-\pi^*$ ( $S_1$ ) and  $^1\pi-\pi^*$ ( $S_2$ ) absorption bands peak at 340

and 260 nm respectively in CD<sub>3</sub>CN compared to 305 and 260 nm in D<sub>2</sub>O). If we take the ab initio calculations as a reference for the gas-phase energies, the <sup>1</sup>n-π (S<sub>1</sub>) state of NMTAA is shifted by 1600 cm<sup>-1</sup> in acetonitrile and by 5500 cm<sup>-1</sup> in water while the <sup>1</sup>π-π\* (S<sub>2</sub>) state is essentially unshifted with respect to the ground state because of a very similar dipole moment. To a first approximation we may assume that the solvation shifts of n-π\* and π-π\* states are similar for triplet and singlet states. Thus, given the ab initio splitting between <sup>3</sup>n-π\* and <sup>3</sup>π-π\* states of about 1000–1500 cm<sup>-1</sup>, the <sup>3</sup>π-π\* state would indeed be well below the <sup>3</sup>n-π\* state in water, while the two states would have almost identical energies in acetonitrile. However, for a quantitative agreement with the infrared data, triplet-triplet (<sup>3</sup>ππ\*-<sup>3</sup>nπ\*) and triplet-singlet (<sup>3</sup>nπ\*-S<sub>0</sub>) relaxation would need to take place at almost identical rates in both solvents to explain why approximately the same number of molecules follow the fast and the slow relaxation channel to the electronic ground state upon S<sub>2</sub> excitation.

This makes us believe that one should not completely neglect the constraints imposed by the conical intersections or intersystem crossing points, which define the molecular geometries for which the electronic energy surfaces become close enough for efficient population transfer. The ab initio calculations<sup>4</sup> suggest that the (four) conical intersections between S<sub>0</sub> and S<sub>1</sub> or the four intersystem crossing points between S<sub>0</sub> and triplet states are energetically above the minima of the respective excited electronic states. Thus, fast relaxation to the electronic ground state may be limited upon direct S<sub>1</sub> excitation because the molecules do not have enough excess energy to directly access CIs or intersystem crossing points. In contrast, molecules that are initially prepared in the S<sub>2</sub> state can give rise to a highly thermally excited S<sub>1</sub> or triplet population with enough kinetic energy to follow directly into the S<sub>1</sub>/S<sub>0</sub> conical intersections or T<sub>n</sub>/S<sub>0</sub> intersystem crossing points. The remaining population in the excited state may get trapped either in the S<sub>1</sub> or the lowest lying triplet state. Within this scenario, which of these excited states is finally populated or the ordering of the triplet states may not be critical to explain the presence of fast and slow relaxation to the electronic ground state. However, due to the much larger S<sub>2</sub>-S<sub>1</sub> energy gap in acetonitrile more excess energy than in water should be available for fast relaxation to the electronic ground state. We may thus expect a larger portion of the population to reach the ground state on the faster time scale in acetonitrile, in contrast to the very similar dynamics for both solvents in Figure 3, parts b and c. It is possible that the crossing point geometries and the relaxation pathway among the electronically excited states change significantly due to the different solvent shifts of π-π\* and n-π\* states, or indeed, an inversion of the triplet state ordering in water leads to very similar energy gaps between S<sub>2</sub> and the lowest lying excited state of NMTAA in both solvents. Clearly, to establish the exact role of the excited states in the fast isomerization dynamics, additional experimental information is required.

The visible pump-probe data (ref 5) indicate that the 4 ps rise time of the excited-state absorption band of NMTAA is associated with a blue-shift, which could be caused by thermal relaxation in the excited state. This shift (and the 4 ps time constant) is absent in the larger peptides, where intramolecular energy redistribution may be faster.<sup>5</sup> Thus, it can be speculated that faster intramolecular energy redistribution in larger thiopeptides with more internal degrees of freedom will reduce the probability of fast relaxation to the electronic ground state and, in the extreme case, lead to a trapping of all molecules in the electronically excited state for a few 100 ps.

One may argue that geometric constraints imposed by the conical intersections or CIs would prevent a blocked molecule like CTA to efficiently relax to the ground state.<sup>5</sup> However, the five-membered ring, which locks CTA in the “cis” form, should still allow the molecule to access the CI or ISC that leads back to the cis-ground state. In NMTAA these are characterized by the pyramidalization of the carbon and nitrogen centers, a S-C-N angle close to 90° and a torsional C-C-N-C angle of only 50°.<sup>4</sup> Furthermore, the importance of molecular geometry in the relaxation of photoexcited NMTAA is underlined by the observation of phosphorescence when the molecule is excited in a low-temperature methanol/ethanol glass.<sup>6</sup> Most likely the rigid glass environment prevents pyramidalization in the electronically excited state which causes this dramatic increase in excited-state lifetime. (Note that for NMTAA dissolved in liquid methanol and ethanol at room-temperature we observe similar dynamics as in water and acetonitrile—data not shown).

The notion that the energetics of the crossing points and a diffusive search, rather than the orbital character of the excited states determine the relaxation to the ground-state once the cooling process in the excited state is completed is consistent with the observation that the slow time scale for ground-state recovery is independent of the initial configuration of the molecule (cis or trans), identical for S<sub>1</sub> and S<sub>2</sub> excitation and very similar in water and acetonitrile. This suggests that the same electronically excited-state acts as a bottleneck in all cases. Another indication for the existence of a common intermediate state is given by the sum of the quantum efficiencies for trans-cis isomerization (30–40%) and cis-trans isomerization (60–70%) that is close to unity. The common state is populated from either the trans or the cis conformer and then decays via the same pathways. In NMTAA, diffusion along the torsional coordinate is expected to occur on a similar time scale as the rotational diffusion of the molecule. Therefore, the molecules have plenty of time to sample all torsional angles during the excited state lifetime, which can explain the complete loss of memory of the initially excited conformation.

As an alternative, we consider the possibility that the decision between isomerization of NMTAA or return to its initial conformation is only made in the electronic ground state, while the molecule still has enough energy to overcome the ground state isomerization barrier of approximately 7000 cm<sup>-1</sup>.<sup>4</sup> This mechanism could explain quite naturally, why the isomerization yield for S<sub>2</sub>-excitation is very similar on the slow and fast time scale. However, because of the C=N double-bond character in the ground state, which gives rise to the isomerization barrier, we expect the torsional motion about this bond to be strongly driven and to be no longer diffusion-controlled like on the S<sub>1</sub>, T<sub>1</sub>, or T<sub>2</sub> excited state surfaces. Since the excess energy from electronic decay is dissipated to the solvent relatively quickly the final outcome of the photoreaction should thus strongly depend on the molecule's geometry upon crossing to the S<sub>0</sub> surface, as is also suggested by the ab initio minimum energy path calculations (see Figure 7 in ref 4). This makes it appear much more probable that the common intermediate state on which the outcome of the photoreaction is determined is one of the excited states, which are essentially flat in the torsional coordinate. In particular, for larger secondary thiopeptides, efficient isomerization as reported in ref 15 is very unlikely to occur without being predetermined on one of the electronically excited-state surfaces.

## Conclusion

In summary, our time-resolved IR-study shows that the trans and cis quantum yields in the photoisomerization of NMTAA do not depend on the initial configuration of the molecule or the solvent and are very similar for  $S_2$  and  $S_1$  excitation. This strongly suggests a common intermediate state,  $S_1$  or, more likely, the lowest-lying triplet state, on which the outcome of the photoreaction is determined. According to ab initio calculations published earlier<sup>4</sup>  $S_1$ ,  $T_1$ , and  $T_2$  are essentially flat along the isomerization coordinate and energy is required to reach the conical intersections or intersystem crossing points to the electronic ground state. Thus, once the excess energy from photoexcitation is dissipated, relaxation back to the ground state should be essentially diffusion-controlled. In line with this interpretation is our second observation that a well-defined fast component in the ground state relaxation of NMTAA is only present for  $S_2$  but not for  $S_1$  excitation. On the fast time scale, the ground state could be accessed with the excess energy available from  $S_2$  decay. However, a fast intersystem crossing pathway via the  $^3n-\pi^*$  state, which is bypassed upon  $S_1$  excitation cannot be excluded. The proposed isomerization mechanism implies that larger secondary thiopeptides can undergo photoisomerization as long as there are little constraints to the diffusion about the thioamide (essentially single) bond in the electronically excited state due to neighboring residues. For the same reason we expect more rigid secondary structure elements to be broken less efficiently by UV-excitation of a thiopeptide unit.

**Acknowledgment.** We thank Luca de Vico and Massimo Olivucci for fruitful discussions. This work was supported by the Swiss National Science Foundation (SNF) under Contract Number 200020-107492/1.

## References and Notes

- (1) Schutkowski, M.; Frank, R.; Jakob, M.; Thuncke, F.; Fischer, G.; Schutkowski, M. *Angew. Chem., Int. Ed.* **2000**, *39*, 1120.
- (2) Zhao, J.; Micheau, J.-C.; Vargas, C.; Schiene-Fischer, C. *Chem.—Eur. J.* **2004**, *10*, 6093–6101.
- (3) Seebach, D.; Ko, S. Y.; Kessler, H.; Köck, M.; Reggelin, M.; Schmieder, P.; Walkinshaw, M. D.; Bölsterli, K. J.; Bevec, D. *Helv. Chim. Acta* **1991**, *74*, 1953–1990.
- (4) Helbing, J.; Bregy, H.; Bredenbeck, J.; Pfister, R.; Hamm, R. H. P.; Wachtveitl, J.; Vico, L. D.; Olivucci, M. *J. Am. Chem. Soc.* **2004**, *126*, 8823–8834.
- (5) Satzger, H.; Root, C.; Gilch, P.; Zinth, W.; Wildemann, D.; Fischer, G. *J. Phys. Chem. B* **2005**, *109*, 4770–4775.
- (6) Harada, I.; Tasumi, M. *Chem. Phys. Lett.* **1980**, *70*, 279–282.
- (7) Ataka, S.; Takeuchi, H.; Harada, I.; Tasumi, M. *J. Phys. Chem.* **1984**, *88*, 449–451.
- (8) Kato, C.; Hamaguchi, H.; Tasumi, M. *J. Phys. Chem.* **1985**, *89*, 407.
- (9) Bredenbeck, J.; Hamm, P. *Rev. Sci. Instrum.* **2003**, *74*, 3188–3189.
- (10) Hamm, P.; Kaendl, R. A.; Stenger, J. *Opt. Lett.* **2000**, *25*, 1798–1800.
- (11) Holz, M.; Mao, X. A.; Seiferling, D.; Sacco, A. *J. Chem. Phys.* **1996**, *104*, 669–679.
- (12) Moog, R. S.; Ediger, M. D.; Boxer, S. G.; Fayer, M. D. *J. Phys. Chem.* **1993**, *97*, 1496–1501.
- (13) Hamm, P.; Ohline, S. M.; Zinth, W. *J. Chem. Phys.* **1997**, *106*, 519–529.
- (14) El-Sayed, M. A. *J. Chem. Phys.* **1963**, *38*, 2834–2838.
- (15) Zhao, J.; Wildemann, D.; Jakob, M.; Vargas, C.; Schiene-Fischer, C. *Chem. Commun.* **2003**, 2810–2811.